

1 **Raman Spectroscopy identifies differences in ochronotic and non-ochronotic cartilage; a**
2 **potential novel technique for monitoring ochronosis.**

3 Adam M Taylor¹, Daniel D Jenks¹, Vishnu D Kammath¹, Brendan P Norman², Jane P Dillon²,
4 James A Gallagher², Lakshminarayan R Ranganath³, Jemma G Kerns¹.

5 ¹Lancaster Medical School, Faculty of Health & Medicine, Lancaster University, Bailrigg,
6 Lancaster, UK.

7 ²Department of Musculoskeletal Biology, Institute of Ageing and Chronic Disease, University
8 of Liverpool, Liverpool, UK.

9 ³Department of Clinical Biochemistry and Metabolic Medicine, Liverpool Clinical Laboratories,
10 Royal Liverpool University Hospital, Liverpool, UK

11 Email:

12 Adam M Taylor – a.m.taylor@lancaster.ac.uk

13 Daniel D Jenks – d.jenks@lancaster.ac.uk

14 Vishnu D Kammath - v.kammath@lancaster.ac.uk

15 Brendan P Norman – Brendan.Norman@liverpool.ac.uk

16 Jane P Dillon – dillon@liv.ac.uk

17 James A Gallagher – jag1@liv.ac.uk

18 Lakshminarayan R Ranganath – lrang@liv.ac.uk

19 Jemma G Kerns – j.kerns@lancaster.ac.uk

20 Author for correspondence:

1 Dr Adam Taylor

2 Lancaster Medical School, Furness College,

3 Lancaster University,

4 Bailrigg,

5 Lancaster LA1 4YG

6 T: +441524593131

7 E: a.m.taylor@lancaster.ac.uk

8 Word Count: 3543

9 Number of Figures: 4+1 Supplementary

10 Number of Tables 1

11

12

13

14

15

16

17

18

19

1 **Abstract**

2 **Objective**

3 Alkaptonuria (AKU) is a rare, inherited disorder of tyrosine metabolism, where patients are
4 unable to breakdown homogentisic acid (HGA), which increases systemically over time. It
5 presents with a clinical triad of features; HGA in urine, ochronosis of collagenous tissues, and
6 the subsequent ochronotic arthritis of these tissues. In recent years the advance in the
7 understanding of the disease and the potential treatment of the disorder looks promising
8 with the data on the efficacy of nitisinone. However, there are limited methods for the
9 detection and monitoring of ochronosis *in vivo*, or for treatment monitoring.

10 The study aim was to test the hypothesis that Raman spectra would identify a distinct
11 chemical fingerprint for the non-ochronotic, compared to ochronotic cartilage.

12 **Design:**

13 Ochronotic and non-ochronotic cartilage from human hips and ears were analysed using
14 Raman spectroscopy.

15 **Results:**

16 Non-ochronotic cartilage spectra were similar and reproducible and typical of normal articular
17 cartilage. Conversely, the ochronotic cartilage samples were highly fluorescent and displayed
18 limited or no discernible Raman peaks in the spectra, in stark contrast to their non-ochronotic
19 pairs. Interestingly, a novel peak was observed associated with the polymer of HGA in the
20 ochronotic cartilage that was confirmed by analysis of pigment derived from synthetic HGA.

21 **Conclusion:**

1 This technique reveals novel data on the chemical differences in ochronotic compared with
2 non-ochronotic cartilage, these differences are detectable by a technique that is already
3 generating *in vivo* data and demonstrates the first possible procedure to monitor the
4 progression of ochronosis in tissues of patients with AKU.

5 **Keywords:** Alkaptonuria, Ochronosis, Arthropathy, Raman Spectroscopy, Osteoarthritis,
6 Cartilage

7 **Running Headline:**

8 Raman Spectroscopy detects ochronosis

9

Author Accepted Manuscript

1 Introduction

2 Alkaptonuria (AKU) is a rare autosomal recessive disorder of tyrosine metabolism. The
3 condition affects 1 in 250,000-500,000 people and results from the absence of the enzyme
4 homogentisate 1,2-dioxygenase (HGD). This enzyme undertakes the highly specific process of
5 cleaving the benzene ring of homogentisic acid (HGA) to produce maleylacetoacetic acid¹. The
6 condition presents with a triad of clinical features; the first and earliest, presenting from birth,
7 is homogentisic aciduria, which darkens on exposure to air, or on addition of alkali. The
8 second is ochronosis of collagenous tissues, such as the pinna, sclera and articular cartilages
9 of weight bearing joints, usually seen in the third decade of life, but it is unclear exactly when
10 this commences. The third and final feature is ochronotic osteoarthropathy, which usually
11 manifests in the 4th decade of life and affects larger weight-bearing joints that have been
12 subject to many years of ochronosis². There is still no approved treatment for AKU, but
13 nitisinone has shown excellent capacity for preventing HGA, the causative molecule in the
14 condition, building up³ and is completely effective at inhibiting ochronosis in AKU mice⁴. A
15 recent study has shown that nitisinone arrests ochronosis and decreases rate of progression
16 of Alkaptonuria in patients⁵. The effectiveness of nitisinone has shown no adverse effects on
17 osteoarticular cells but can cause corneal opacities, which reverse following withdrawal of
18 the drug^{6,7}.

19 For patients who have long term established ochronosis the only treatment is joint
20 replacement surgery; however, this shows high variability within a patient and between
21 patients, as not all joints progress to this state at the same rate⁸. The reasons for this are still
22 to be fully understood, but it has been suggested that local inflammation, damage or other
23 factors may contribute⁹.

1 The process of ochronosis in collagenous tissues has been shown to disrupt the
2 molecular/atomic structure of type II collagen¹⁰. Most recently glycosaminoglycans (GAGs)
3 have been shown to be absent or not extractable from macroscopically ochronotic cartilage¹¹.
4 The changes that occur in the extracellular matrix of ochronotic cartilage change both the
5 mechanical and biochemical properties⁸. Whilst there has been an advance in the
6 understanding of AKU, it is still unclear when ochronosis starts and whether the process can
7 be reversed *in vivo*. One of the most accessible and easily observable areas that becomes
8 pigmented is the pinna, which can therefore be used for monitoring ochronosis over time.
9 However, although visual estimates are possible, the most accurate measure of ochronosis is
10 a biopsy, which can be painful and potentially disfiguring.

11 Raman spectroscopy is a non-destructive technique that provides a chemically specific
12 signature of a given sample. It has a broad range of applications but is used extensively to
13 probe the chemistry of *in vitro* and *ex vivo* human samples from a range of pathologies¹².
14 Furthermore, in recent years numerous techniques have emerged and been developed that
15 will allow and support *in vivo* measurements¹³. As a laser-based technology it uses a specific
16 monochromatic wavelength to excite molecular bonds in a given sample. Following the
17 molecular vibration, the photons are, either, released at the same energy and wavelength
18 (Rayleigh scattering), or an exchange in energy occurs and the photons released have either
19 lost or gained energy, resulting in a wavelength shift; this is known as Raman scattering, and
20 specific to the energy of the molecular bonds. Therefore, it enables the acquisition of a
21 specific Raman signature or fingerprint of a given material by characterising the chemical
22 bonds within it. Compared to current clinical diagnostic techniques for bone disorders, Raman
23 spectroscopy has some advantages as it can provide information on both the inorganic and
24 organic material present, and is non-ionising¹⁴. An example of the potential for bone disease

1 diagnosis is osteogenesis imperfecta, a collagen disorder, which can be identified *ex vivo* and
2 *in vivo* using Raman spectroscopy¹⁵. It has also been used *ex vivo* to identify osteoarthritis¹⁶
3 and there is some evidence that it may be useful for identifying osteoporosis^{13,18}.
4 Furthermore, chemical differences have been found with AKU cartilage samples using Fourier
5 transform infrared spectroscopy, a technique complementary to Raman spectroscopy, but
6 which does not lend itself to clinical applications due to its sensitivity to water²⁰. The aim of
7 this study is to investigate the chemical composition and potential differences in ochronotic
8 and non-ochronotic cartilage using Raman spectroscopy.

9 **Methods**

10 **Materials**

11 **Hip cartilage samples**

12 Hip cartilage samples, (n=3 pairs (pigmented and non-pigmented)) were obtained as surgical
13 waste with informed patient consent following ethical approval by Liverpool REC
14 (07/Q1505/29). The samples were dissected immediately following surgery into ochronotic
15 and non-ochronotic pairs and stored unfixed at -80°C.

16 **Ear cartilage biopsy**

17 Ear biopsy samples (n=27; aged 16-67 years, 12 males and 15 females, equal males and
18 females within each age group) were obtained, with ethical approval from Preston REC
19 (15/NW/0749), as part of the Subclinical Ochronotic Features In Alkaptonuria (SOFIA) study;
20 patient characteristics given in Table 1.

21 **Ear Visual Ochronosis Score**

1 Ear visual ochronosis score was undertaken by a single blinded scorer, this was performed as
2 part of the Subclinical Ochronotic Features in Alkaptonuria (SOFIA) study where pigmentation
3 across both ears of a single patient was measured. Ears were classified into 1 of 4 groups as
4 having none (0), slight (1), moderate (2) or marked (3) pigmentation. The scores from each
5 ear were combined to give the overall ear visual ochronosis score. We have added a
6 supplementary figure (Suppl. Fig 1) to demonstrate the 4 groups. Ear biopsy % ochronosis
7 score

8 A 4mm diameter biopsy was taken from the conchal bowl of the ear using a posterior
9 approach under local anaesthetic. A single stitch was used at the end of the ear biopsy. The
10 biopsy was fixed in a 4% solution of formaldehyde in phosphate buffered saline for 48 hours
11 and then transferred to a solution of 70% ethanol in water.

12 Each biopsy contained a disc of cartilage 4mm in diameter and 1-2 mm thick. The disc was
13 bisected along the diameter and a thin slice of 0.8mm was taken from the cut face. This
14 sample was examined using an Olympus SZH binocular microscope in darkfield mode at 7.5 X
15 magnification. The biopsy section was photographed using a 9M pixels DCM 900 camera and
16 images stored as TIFFS. TIFFs were opened in Image J as 8-bit RGB images. An oval region of
17 interest 3 mm long by 1 mm wide was selected and the mean colour intensity in the blue
18 channel was quantified on 255 scale, transformed so that white = 0 and black = 255. Following
19 subtraction of the absorbance of non-ochronotic tissue the % absorbance was calculated
20 (non-ochronotic tissue = 0 and completely ochronotic tissue =100), which provided an ear
21 biopsy % ochronosis score. Presence of ochronotic pigmentation was confirmed by histology
22 on serial sections followed by Schmorl staining and microscopy (data not shown).

23 Sample Preparation

1 For analysis via Raman, individual cartilage samples were placed onto an inert calcium fluoride
2 (CaF₂) disc for analysis. Samples were secured using clingfilm, with a hole where
3 measurements were taken, which also ensured the samples did not dry out during spectral
4 acquisition.

5

6 Instrumentation

7 Raman spectra were acquired from the samples using an InVia Raman microspectrometer
8 (Renishaw plc, Gloucestershire, UK), equipped with a 785 nm laser, 200 mW at source, ~10
9 mW at sample. A minimum of five spectra were collected from each sample, all spectra were
10 acquired in the spectral range 600 – 1700 cm⁻¹. Spectral resolution was 1 cm⁻¹.

11 Hip sample spectral acquisition and processing

12 Spectra were collected over 60 s (20 s x 3 accumulations), at 100% power, from the non-
13 ochronotic tissue. However, applying the same settings to the ochronotic tissue resulted in
14 detector saturation. Therefore, spectra were collected over 10 s (1 s x 10 accumulations), at
15 100 % power, from the ochronotic tissue. This setting was also tested on the non-ochronotic
16 sample but resulted in spectra with a very low signal to noise (S/N) ratio. Data were baseline
17 corrected, using polynomial (order 5) subtraction, to remove fluorescence and normalised to
18 the phenylalanine peak (1000 cm⁻¹). A further liquid sample of pure HGA polymer,
19 synthesised in the lab, was analysed with a drop placed on the disk. The polymer was analysed
20 to help identify a characteristic Raman spectrum that might have been present in the tissue
21 samples. Six spectra were acquired at 50% power for 60 s (1 s x 60 accumulations); higher
22 power resulted in detector saturation.

1 Ear sample spectral acquisition and processing

2 To acquire spectra from the majority of the samples, i.e., to avoid detector saturation from
3 the highly ochronotic regions, while collecting good quality S/N from the non-ochronotic
4 regions the spectra were collected over 5 s (1s x 5 accumulations) at 50 % power, with cosmic
5 ray removal turned on. Spectra were collected every 200 μm across the longest axis of each
6 sample (samples were ellipsoidal in shape), with a minimum of 15 spectra per sample. 448
7 spectra were collected in total, 44 were saturated, leaving a total of 404 spectra for analysis.

8 All spectra were baseline corrected using a 5th polynomial subtraction and vector normalised
9 using an in-house written Matlab (v2017a, The Mathworks, Inc., Natick, MA, USA) script.

10 Principal component analysis (PCA) and PCA-linear discriminant analysis (PCA-LDA) was then
11 performed on this data. Data were grouped by ear ochronosis and ear pigmentation scores,
12 and by degree of fluorescence in the raw spectra. The latter, with PCA, was used to enable a
13 'blind' and unsupervised approach to identify natural variation in the Raman spectral data.

14 A fluorescence to Raman ratio was calculated by comparing the peak height of the raw
15 intensity (counts on y-axis) to baselined spectra at 783 cm^{-1} . This peak was chosen as it was
16 consistently present in the spectra and was identified as contributing to differences between
17 non-ochronotic and ochronotic samples from PCA-LDA. As the ochronotic samples were
18 highly fluorescent the area under the curve was calculated for each raw spectrum to provide
19 a measure of the amount of fluorescence.

20 Results

21 Hip samples

1 The average spectrum from each of the non-ochronotic samples is presented in Figure 1A; it
2 can be observed by eye that they are similar and reproducible. FIGURE 1 LOCATED HERE

3 Raw spectra acquired from the ochronotic samples are presented in Figure 1B; they are
4 remarkably similar to each other. The strongest feature of these spectra is that they reveal a
5 high degree of fluorescence and do not contain easily identifiable peaks that are comparable
6 to either the non-ochronotic cartilage or the cartilage spectra in the literature. Upon baseline
7 correction (Figure 1C) it was possible to identify several peaks, although the quality of the
8 spectra is poor. The main peaks identified were at 626 cm^{-1} , 775 cm^{-1} and 1675 cm^{-1} .

9 The synthesised HGA polymer produced similar results to the ochronotic samples, in that the
10 spectra showed high levels of fluorescence and with 100% power resulted in detector
11 saturation. Upon baseline correction (Figure 1D), peaks were identifiable, the largest and
12 most distinct at 1675 cm^{-1} , with others at 1072 cm^{-1} and a broad band at 1310 cm^{-1} .

13 Ear Samples

14 As with the non-ochronotic spectra from the hip cartilage, the equivalent from the ear
15 samples also provided spectra that had clearly identifiable spectral bands, and a different
16 fluorescence profile to the ochronotic samples, which were highly fluorescent (Figure 2A).
17 Once processed the Raman spectral profiles were more comparable to non-ochronotic
18 spectral profiles (Figure 2B). FIGURE 2 LOCATED HERE

19 The fluorescence, as determined by the area under the curve, was strongly correlated with
20 both the visual ear ochronosis score ($R^2= 0.73$; Figure 3A) and the ear biopsy % ochronosis
21 score ($R^2= 0.63$; Figure 3B). Of the samples, one in particular had clearly defined ochronotic
22 and non-ochronotic regions (Figure 3C), the spectral ratio of fluorescence to Raman (raw

1 divided by baseline corrected peak height at 783 cm^{-1}) signal clearly maps onto the image;
2 specifically, regions of high ochronosis have a higher fluorescence to Raman ratio (Figure 3D).
3 Of note is that the darker regions on the right of the sample (Figure 3C) resulted in spectra
4 that were saturated, so we hypothesise that had they been measurable the fluorescence
5 would have been higher from point 12-16 (Figure 3D). FIGURE 3 LOCATED HERE

6 In a PCA scores plot the closer two scores are to each other the more similar they are
7 spectrally, and therefore biochemically, and vice versa. Figure 4A demonstrates that there is
8 a clear separation in the PCA scores plot between samples classified as non-ochronotic
9 compared to ochronotic. There is some overlap of the 95% confidence intervals, however,
10 this is likely because some of the samples contained regions that were both ochronotic and
11 non-ochronotic, such as the one shown in Figure 3C. This is further demonstrated in the PCA-
12 LDA scores plot of the same data (Figure 4B); this 1D plot shows that the most ochronotic
13 spectrum is furthest to the right. The loadings plot (Figure 4C) reveals that the spectral, and
14 therefore biochemical, reason for the separation is primarily due to variation at 783 cm^{-1}
15 (collagen), 879 cm^{-1} (tryptophan/hydroxyproline), 718 cm^{-1} (DNA), 886 cm^{-1} (collagen), 1199
16 cm^{-1} (NH_2), 1657 cm^{-1} (carbonyl; $\text{C}=\text{O}$) 1451 cm^{-1} (CH_2) and 1333 cm^{-1} (collagen), 1149 cm^{-1}
17 (NH_2), 976 cm^{-1} (C-H stretch phenylalanine/C-C stretch tryptophan) in order of highest
18 contribution to the variance, to the lowest. FIGURE 4 LOCATED HERE

19 Further analysis (Figure 4D) highlights the spread of individuals' data compared to the data
20 grouped by ochronosis. This not only demonstrates the separation of samples based on
21 ochronosis but also the intra-sample variation, i.e., the heterogeneity of ochronosis within
22 one patient sample.

1 Analysing the Raman spectra with PCA-LDA according to ear biopsy % ochronosis score
2 demonstrates that the samples without ochronosis are distinct from those with at least 60%
3 ochronosis (Figure 4E). The samples with varying degrees of ochronosis appear as a spread
4 across both regions but reveal differences within and between samples.

5

6

Author Accepted Manuscript

1 **Discussion**

2 This study demonstrates the novel application of Raman to the rare genetic disease AKU, its
3 use demonstrates the ability to distinguish clear chemical differences between non-
4 ochronotic and ochronotic cartilage. The ability to demonstrate subtle differences,
5 undetectable by visual methods, using a technique that is already used clinically means that
6 this could be applied to AKU patients *in vivo* for real time monitoring of ochronosis and to
7 determine appropriate time to treat. The spectra from the non-ochronotic samples, hip
8 (hyaline) and ear (elastic) cartilage were comparable to each other and are typical of
9 articular¹⁹ and elastic²¹ cartilage spectra, respectively. The main difference is the presence of
10 elastin fibres, and while a direct comparison of the two cartilage types may identify spectral
11 differences, this is not clear from the raw spectra, and no direct comparisons were made.
12 Although the hip spectra were acquired using 1 min spectra, this setting was the optimal for
13 signal to noise ratio and discernible peaks could be identified on smaller collection times, as
14 observed with 5 s ear spectra. Spectra acquired from the ochronotic cartilage from all the
15 samples produced the same comparable spectra, which were inundated by fluorescence.
16 Furthermore, it was only possible to collect spectra using minimal exposure settings; any
17 higher resulted in detector saturation and therefore no recorded measurement. However,
18 upon baseline correction and normalisation, peaks become recognisable. Of these peaks one
19 was also present on the HGA polymer spectra (1675 cm⁻¹), which is due likely due to yellow
20 chromophores, specifically p-quinone²². This observation presents some of the first evidence
21 of the existence of a quinone-intermediary in the ochronosis process, the exact structure and
22 binding site of this product is still elusive.

1 The HGA polymer is chemically similar to melanin, the pigment found in skin²³. However, as
2 reported in the literature it is possible to acquire distinct spectra from a range of skin types
3 with differing levels of melanin²⁴. The intermediate in the tyrosine to melanin pathway is L-
4 dopaquinone, which is chemically similar to benzoquinone, the intermediate in the
5 polymerisation of HGA. While it may have been hypothesised that high levels of melanin may
6 produce the same results that have been measured with ochronotic tissue, this was not the
7 case. This is very likely due to a difference in the chemical environment. Specifically, melanin
8 is found intracellularly, whereas HGA becomes bound to the extracellular matrix in addition
9 to cellular deposition. Therefore, the combination of small chemical differences and the
10 environment likely explain the very different vibrational fingerprints. One particular feature
11 of the HGA is the large degree to which it fluoresces and is Raman active.

12
13 Fluorescence occurs when there is an overall increase in energy to all the molecules present
14 in a given sample and is a separate and distinct phenomenon to Raman scattering, which
15 provides molecule-specific information. In the majority of Raman spectroscopy studies the
16 first step after acquisition is to remove the fluorescence to leave behind the pure Raman
17 spectrum, it is then necessary to perform analysis, which, as each spectrum can contain ~1000
18 variables, often requires multivariate analysis to identify differences due to the presence of
19 different chemicals, e.g., in disease. Utilising both the fluorescence and Raman information
20 (Figure 3) revealed that differences due to ochronosis could be detected. Specifically, there
21 was a strong exponential trend between fluorescence and both the ear ochronosis (visual)
22 and ear biopsy (ear biopsy % ochronosis) scores. Furthermore, the fluorescence to Raman
23 ratio identified that differences within a sample, due to ochronosis, could be observed; the

1 sample in Figure 3C was so pigmented at one side that the detector saturated for the last 5
2 spectra. It is assumed that the fluorescence to Raman ratio, had it been measurable, would
3 have been higher here. However, the result of a saturated spectrum is a result in itself as it is
4 strongly associated with high pigmentation.

5 AKU is a rare disease, and although there is active research, much is still unknown. Although
6 ochronosis is known to occur, the rate and anatomical location varies and is patient-specific.
7 A technique that could monitor pigmentation, to aid in clinical decision making for treatment
8 and in monitoring treatment efficacy would be very valuable. Its most significant use would
9 be the ability to determine the exact time point when an individual should commence
10 nitisinone therapy. This technique has revealed that the presence, or absence, of ochronosis
11 could be identified by measuring fluorescence. Therefore, potentially a visible light source
12 may provide similarly useful information. However, Raman has the added value of providing
13 chemical information. The results shown in Figure 4 have provided insight into the intra-class,
14 intra-sample and inter-class variation. A comparison of the Raman data to the ear biopsy %
15 ochronosis showed a strong correlation for non-ochronotic and ochronotic cartilage, with
16 overlap in between. This is perhaps expected due to the difference in measurements and the
17 heterogeneous nature of the samples, specifically once ochronosis has started. Furthermore,
18 the biochemical differences between the ochronotic and non-ochronotic samples are due to
19 changes in collagen spectral bands, specifically hydroxyproline, amide groups and
20 phenylalanine/tryptophan which gives indication as to the association with the pigment and
21 extracellular binding sites, similar to those already identified¹⁰. Therefore, the technique is
22 providing information about the underlying chemical changes due to the pigmentation, as
23 well as the presence and relative amount of ochronosis.

1 Overall, the spectra acquired from the non-ochronotic and ochronotic samples are distinctly
2 different at the point of data collection, suggesting that the Raman technique can be used to
3 sensitively detect ochronosis and monitor its progression. Therefore, this has the potential to
4 be a powerful *in vivo* diagnostic tool for AKU. The limitations of this study include a small
5 sampling aperture; future studies would benefit from using an image map analysis approach
6 or a smaller magnification objective, the latter of which may allow a higher power laser to be
7 used. The advantage of this investigation is that although AKU is a rare disease, we were able
8 to collect ear biopsy data from a significant number of participants, and from a range of
9 disease stages. The technique of Raman spectroscopy is already available in a clinical setting
10 to measure bone transcutaneously, albeit in the early trial stages, for osteoporosis¹⁸,
11 osteoarthritis and osteogenesis imperfecta¹⁵. The technique lends itself to a clinical setting as
12 it benefits from the advantages of being non-invasive and non-ionising, it has also been used
13 to generate distinct spectra from other areas of the body containing connective tissue²⁵. The
14 promising benefits of nitisinone for treating AKU is not without its side effects, this technique
15 would enable targeted treatment of patients with this drug by monitoring sites of superficial
16 ochronosis in sites such as the ear, Achilles tendon or patella tendon. Overall, this technique
17 has the potential to be used routinely in clinics for the diagnosis, monitoring and treatment
18 efficacy of individuals with AKU with no adverse health risks.

19 **Author contributions**

20 AMT, JGK, JAG & LRR conceived and designed the study. VDK, DDJ and BN collected samples
21 and undertook data acquisition. JPD processed the ear cartilage biopsies and undertook data
22 acquisition. All authors analysed and interpreted the data, contributed to drafting the
23 manuscript and revising it critically for important intellectual content.

1 **Funding support:** This work was supported by the EU, the Rosetrees Trust, AKU Society, Royal
2 Liverpool University Hospital and the Pathological Society. Ear biopsies were collected of was
3 part of the SOFIA (Subclinical Ochronosis Features In Alkaptonuria) a study supported by
4 European Commission Seventh Framework Programme funding granted in 2012
5 (DevelopAKUre, project number: 304985).

6 **Disclosures:**

7 All authors have no disclosures in relation to this manuscript.

8

9 **References**

- 10 1. Mistry JB, Bukhari M, Taylor AM. Alkaptonuria. Rare Dis. 2013 Dec 18;1:e27475
- 11 2. Helliwell TR, Gallagher JA, Ranganath L. Alkaptonuria--a review of surgical and
12 autopsy pathology. Histopathology. 2008 Nov;53:503-12
- 13 3. Ranganath LR, Milan AM, Hughes AT, Dutton JJ, Fitzgerald R, Briggs MC, et al.
14 Suitability Of Nitisinone In Alkaptonuria 1 (SONIA 1): an international, multicentre,
15 randomised, open-label, no-treatment controlled, parallel-group, dose-response
16 study to investigate the effect of once daily nitisinone on 24-h urinary homogentisic
17 acid excretion in patients with alkaptonuria after 4 weeks of treatment. Ann Rheum
18 Dis. 2016 Feb;75(2):362-7
- 19 4. Preston AJ, Keenan CM, Sutherland H, Wilson PJ, Wlodarski B, Taylor AM, et al.
20 Ochronotic osteoarthropathy in a mouse model of alkaptonuria, and its inhibition by
21 nitisinone. Ann Rheum Dis. 2014;73:284-9.

- 1 5. Ranganath LR, Khedr M, Milan AM, Davison AS, Hughes AT, Usher JL, et al. Nitisinone
2 arrests ochronosis and decreases rate of progression of Alkaptonuria: Evaluation of
3 the effect of nitisinone in the United Kingdom National Alkaptonuria Centre. *Mol*
4 *Genet Metab.* 2018 Sep;125(1-2):127-134
- 5 6. Mistry JB, Jackson DJ, Bukhari M, Taylor AM. Osteoarticular cells tolerate short-term
6 exposure to nitisinone-implications in alkaptonuria. *Clin Rheumatol.* 2016
7 Feb;35(2):513-6.
- 8 7. Khedr M, Judd S, Briggs MC, Hughes AT, Milan AM, Stewart RMK, et al.
9 Asymptomatic Corneal Keratopathy Secondary to Hypertyrosinaemia Following Low
10 Dose Nitisinone and a Literature Review of Tyrosine Keratopathy in Alkaptonuria.
11 *JIMD Rep.* 2017 Sep 24.
- 12 8. Taylor AM, Boyde A, Wilson PJ, Jarvis JC, Davidson JS, Hunt JA, et al. The role of
13 calcified cartilage and subchondral bone in the initiation and progression of
14 ochronotic arthropathy in alkaptonuria. *Arthritis Rheum.* 2011 Dec;63:3887-96
- 15 9. Mistry JB, Jackson DJ, Bukhari M, Taylor AM. A role for interleukins in ochronosis in a
16 chondrocyte in vitro model of alkaptonuria. *Clin Rheumatol.* 2016 Jul;35(7):1849-56.
- 17 10. Chow WY, Taylor AM, Reid DG, Gallagher JA, Duer MJ. Collagen atomic scale
18 molecular disorder in ochronotic cartilage from an alkaptonuria patient, observed by
19 solid state NMR. *J Inherit Metab Dis.* 2011 Dec;34:1137-40.
- 20 11. Taylor AM, Hsueh MF, Ranganath LR, Gallagher JA, Dillon JP, Huebner JL, et al.
21 Cartilage biomarkers in the osteoarthropathy of alkaptonuria reveal low turnover
22 and accelerated ageing. *Rheumatology (Oxford).* 2017 Jan;56(1):156-164.

- 1 12. Butler HJ, Ashton L, Bird B, Cinque G, Curtis K, Dorney J, et al. Using Raman
2 spectroscopy to characterize biological materials. *Nature Protocols*. 2016;11: 664–
3 687.
- 4 13. Matousek P, Draper ERC, Goodship AE, Clark IP, Ronayne KL, & Parker, A. W. Non-
5 invasive Raman spectroscopy of human tissue in vivo. *Central Laser Facility Annual*
6 *Report*. 2006: 133–135.
- 7 14. Morris MD, & Mandair GS. Raman Assessment of Bone Quality. *Clinical Orthopaedics*
8 *and Related Research*. 2010;469: 2160-2169.
- 9 15. Buckley, K, Kerns JG, Gikas PD, Birch HL, Vinton J, Keen R, et al. Measurement of
10 abnormal bone composition in vivo using noninvasive Raman spectroscopy. *IBMS*
11 *BoneKEy*. 2014;11: 602.
- 12 16. Kerns JG, Gikas, PD, Buckley K, Shepperd A, Birch HL, McCarthy I, et al. Evidence from
13 Raman spectroscopy of a putative link between inherent bone matrix chemistry and
14 degenerative joint disease. *Arthritis & Rheumatology (Hoboken, N.J.)*. 2014;66:
15 1237–46.
- 16 17. McCreddie BR, Morris MD, Chen TC, Sudhaker Rao D, Finney WF, Widjaja E, et al.
17 Bone tissue compositional differences in women with and without osteoporotic
18 fracture. *Bone* 2016;39: 1190–5.
- 19 18. Buckley K, Kerns JG, Vinton J, Gikas PD, Smith C, Parker AW, et al. Towards the in vivo
20 prediction of fragility fractures with Raman spectroscopy. *Journal of Raman*
21 *Spectroscopy*. 2015;46: 610-618.
- 22 19. Esmonde-White, K. Raman spectroscopy of soft musculoskeletal tissues. *Applied*
23 *Spectroscopy*. 2014;68: 1203–1218.

- 1 20. Mitri E, Millucci L, Merolle L, Bernardini G, Vaccari L, Gianoncelli A, et al. A new light
2 on Alkaptonuria: A Fourier-transform infrared microscopy (FTIRM) and low energy X-
3 ray fluorescence (LEXRF) microscopy correlative study on a rare disease. *Biochimica
4 et Biophysica Acta - General Subjects*. 2017;1861: 1000–1008.
- 5 21. Green E, Ellis R, & Winlove P. The molecular structure and physical properties of
6 elastin fibers as revealed by Raman microspectroscopy. *Biopolymers*. 2008;89: 931–
7 940.
- 8 22. Agarwal UP. Assignment of the Photoyellowing-Related 1675 cm^{-1} Raman/IR Band
9 to P-Quinones and Its Implications to the Mechanism of Color Reversion in
10 Mechanical Pulps. *Journal of Wood Chemistry and Technology* 1998;18: 381–402.
- 11 23. Roberts NB, Curtis SA, Milan AM, Ranganath LR. The Pigment in Alkaptonuria
12 Relationship to Melanin and Other Coloured Substances: A Review of Metabolism,
13 Composition and Chemical Analysis. *JIMD Rep*. 2015;24:51-66.
- 14 24. Huang Z, Lui H, Chen XK, Alajlan A, McLean DI, & Zeng H. Raman spectroscopy of in
15 vivo cutaneous melanin. *Journal of Biomedical Optics*. 2004;9: 1198.
- 16 25. Pudney PD, Bonnist EYM, Caspers, PJ, Gorce JP, Marriot C, Puppels GJ, et al. A new in
17 vivo Raman probe for enhanced applicability to the body. *Applied Spectroscopy*.
18 2012;66: 882–91.

19

20

21

22

1
2
3
4
5
6
7
8
9
10
11
12
13
14
15
16
17
18
19
20
21

Figures

Figure 1: Raman spectra from ochronotic and non-ochronotic hip cartilage samples from patients with AKU. [A] Average spectrum from each hip sample of non-ochronotic cartilage, baseline corrected and normalised; [B] Average raw spectrum from each sample of ochronotic cartilage; [C] Average spectrum from each sample of ochronotic cartilage, baseline corrected. Blue boxes highlight identifiable peaks; [D] Baseline corrected spectrum of the synthesised HGA polymer. Blue boxes highlight identifiable peaks.

Figure 2: Raman spectra from ear cartilage samples from patients with AKU. Average spectrum from each class of ear sample: non-ochronotic vs ochronotic cartilage (based on observation of the spectra), [A] raw; [B] baseline corrected and normalised.

Figure 3: Comparison of Raman spectroscopy and visual ochronosis assessment in ear cartilage samples from AKU patients. [A] Ear ochronosis score vs. fluorescence; [B] biopsy % ochronosis score vs. fluorescence; [C] image of an example ear sample with defined ochronotic and non-ochronotic regions, red line is the location Raman spectra were acquired along Spectra were acquired every 200 μm . A scale bar is provided; [D] fluorescence to Raman ratio at 783 cm^{-1} related to position along the sample in [C].

1 **Figure 4: PCA of Raman spectroscopy distinguishes between ochronotic and non-**
2 **ochronotic cartilage** [A] PCA scores plot of non-ochronotic (blue circles) vs. ochronotic
3 (black squares) spectra, with 95% confidence ellipses; [B] PCA-LDA scores plot of non-
4 ochronotic (blue circles) vs. ochronotic (black squares) spectra; [C] PCA-LDA loadings plot
5 corresponding to [B], with the labelled peaks showing those that contribute the most; [D]
6 PCA-LDA scores plot of the same data as [B] but with 3 samples worth of spectra classed
7 individually (non-ochronotic, green triangles; a sample with both ochronotic and ochronotic
8 regions (sample image in Figure 3C) red diamonds; ochronotic sample, blue inverted
9 triangles); [E] PCA-LDA scores plot with the data classed by ear biopsy % ochronosis.

10 **Supplementary Figure 1: Photographs showing 4 stages of pigmentation as scored in the**
11 **Ear Visual Ochronosis Score.** [A] Photograph showing an ear with zero pigmentation, scored
12 0. [B] Photograph showing an ear with slight pigmentation, scored 1. [C] Photograph
13 showing an ear with moderate pigmentation, scored 2. [D] Photograph showing an ear with
14 marked pigmentation, scoring 3.

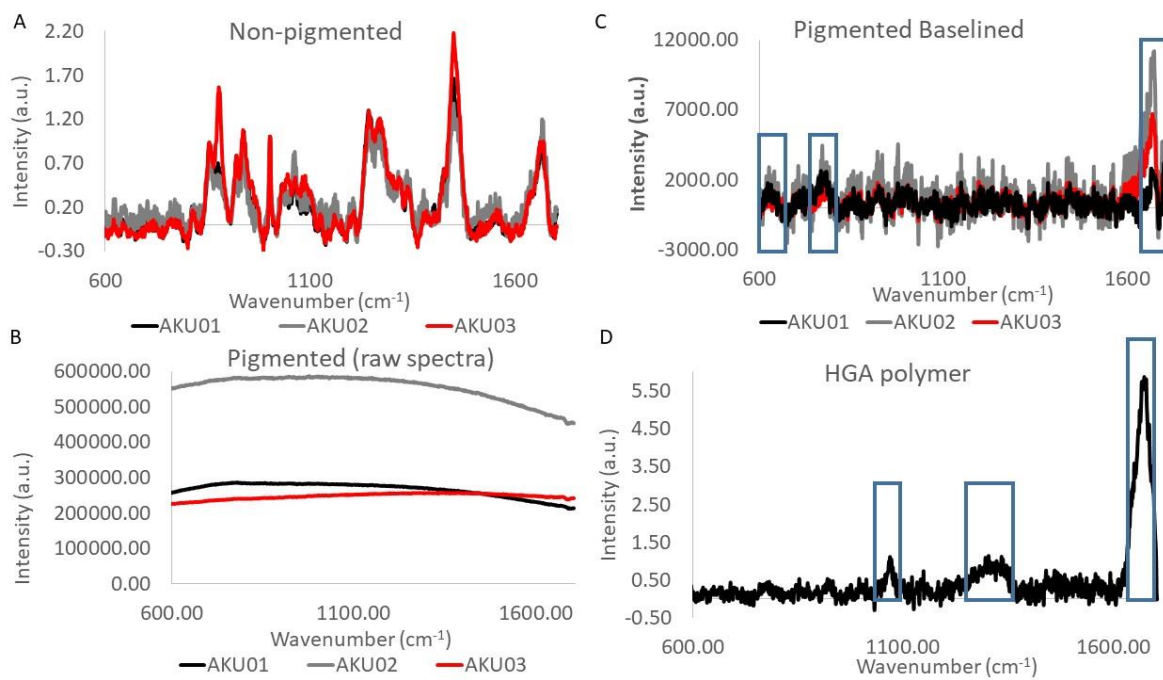
15

1 **Table 1:** Table of patient demographics and their visual and biopsy ochronosis scores

SOFIA			Visual ear ochronosis	Ear biopsy % ochronosis
ID	Age	Gender	score	score
3	62	M	2	60
5	59	F	3	4
6	43	M	3	100
7	46	M	6	99.6
8	36	F	1	29
9	57	M	6	59
10	33	M	0	9
11	34	F	2	0
12	46	F	3	58
13	43	F	0	38
14	67	F	6	81
15	29	F	0	20
16	43	F	4	71
17	33	M	0	0
18	49	M	3	20
19	49	M	3	11
20	37	F	0	44
21	35	F	0	11
22	31	F	0	0
23	20	F	0	29
24	16	M	0	0
25	16	M	0	0
26	26	F	0	0
27	24	F	0	0
28	22	M	0	0
29	23	M	0	0
30	23	F	0	0

2

1 Figure 1

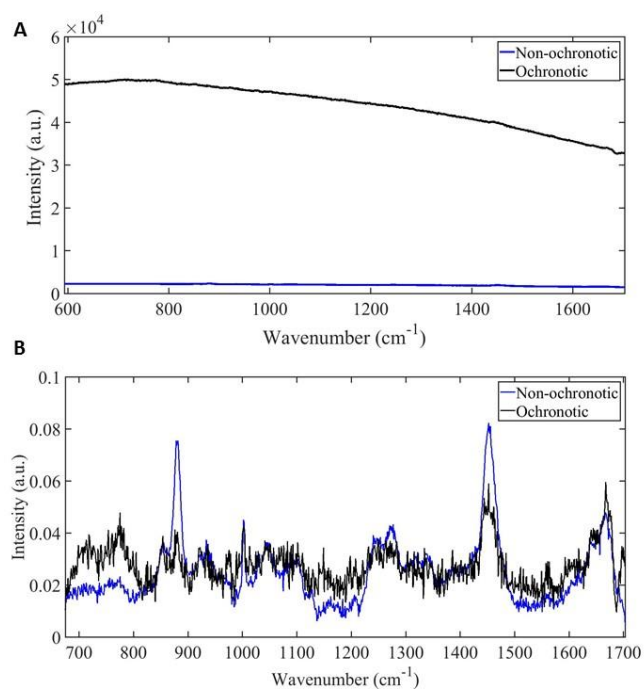


2

3

Author Accepted Manuscript

1 Figure 2



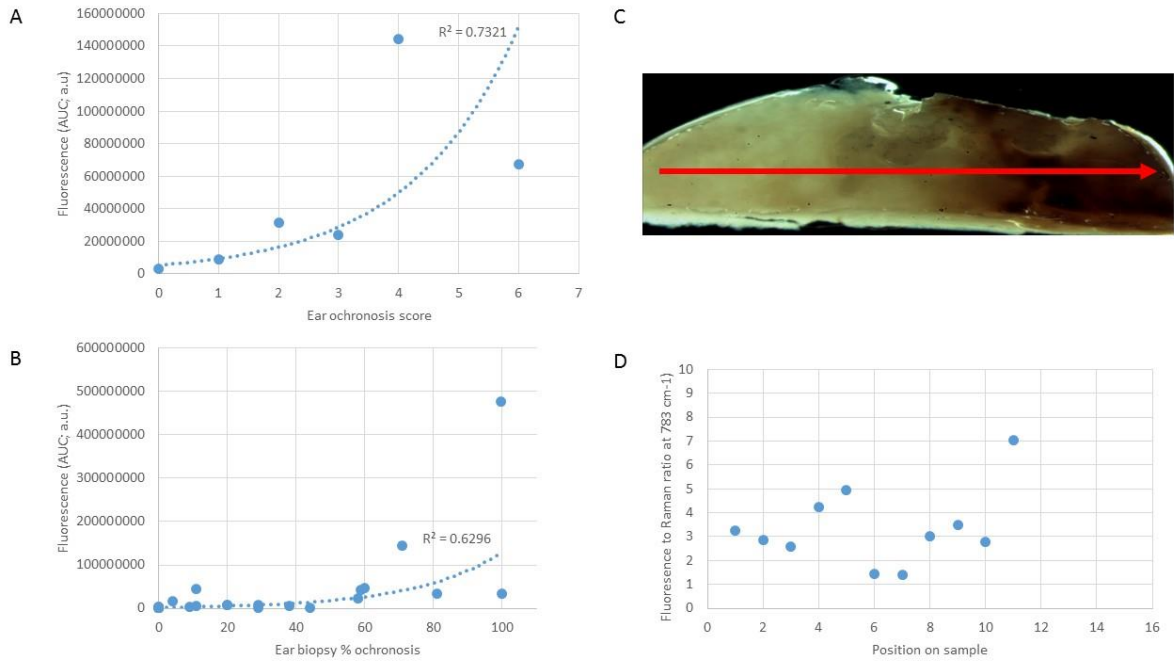
2

3

Author Accepted Manuscript

1 Figure 3

2

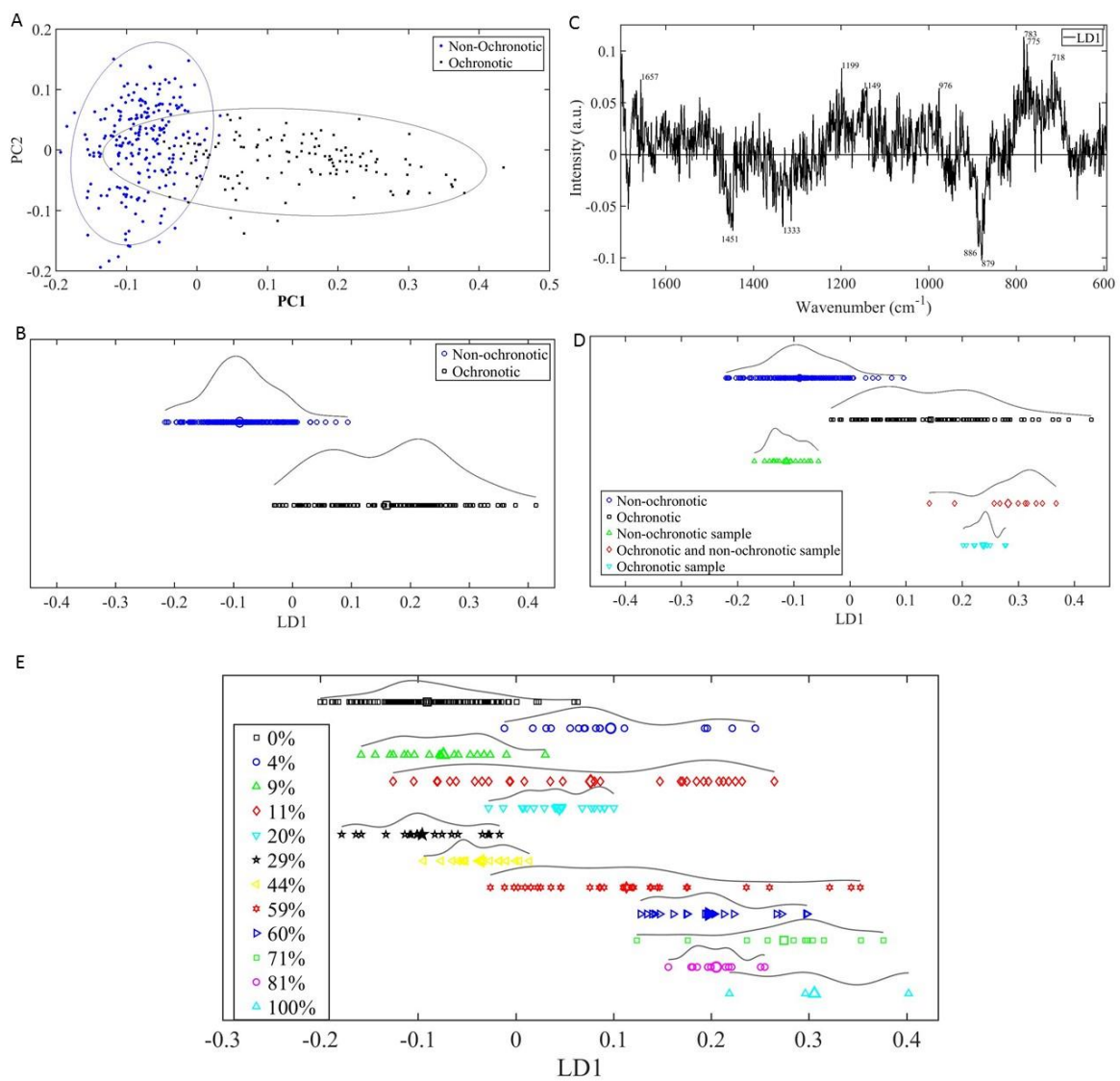


3

4

Author Accepted

1 Figure 4



2